The effect of ischemia – hypoxia in rats on angiogenesis in myofascial trigger points assessed by color Doppler flow imaging

Fangyan Jiang [Equal first author, 1], **Shuangcheng Yu** [Equal first author, 2], **Haiqing Su** [1], **Shangyong Zhu** [Corresp. 3]

[1] Department of Medical Ultrasound, the Affiliated Ethnic Hospital of Guangxi Medical University, Nanning, Guangxi, China

[2] Department of Radiology, the Affiliated Ethnic Hospital of Guangxi Medical University, Nanning, Guangxi, China

[3] Department of Medical Ultrasound, the First Affiliated Hospital of Guangxi Medical University, Nanning, Guangxi, China

Corresponding Author: Shangyong Zhu
Email address: zhushangyong2019@hotmail.com

Background & Aims. Myofascial pain syndrome (MPS) is a common non-articular disorder of the musculoskeletal system which is characterized by the presence of myofascial trigger points (MTrPs). Despite the high prevalence of MPS, its pathogenesis, which induces the onset and maintenance of MTrPs, is still not fully understood. To date, there are no studies investigating the changes in the biochemical milieu with respect to ischemia and hypoxia that mentioned in the integrated hypothesis in the MTrPs region of the muscle. Therefore, this study was to investigate whether ischemia-hypoxic conditions are involved in the formation of MTrPs to affect angiogenesis assessed by color Doppler flow imaging (CDFI). **Methods.** Twenty-five Sprague Dawley rats were randomly divided into a model group and a normal control group. The model of MTrPs was established by a blunt strike combined with eccentric exercise. Enzyme-linked immunosorbent assay (ELISA) analyses were employed to detect the serum levels of HIF-1α and VEGF. Microvessel density (MVD) was evaluated by immunohistochemistry. CDFI was applied to observe the blood flow signals in the MTrPs, which were graded as four types based on their strength. **Results.** Compared with those in the control group, the expression of HIF-1α and VEGF as well as the MVD in the MTrPs group were significantly increased. This was accompanied by increased blood flow signals. In the MTrPs group, the grade of the blood flow signal was positively correlated with the MVD ($P<.05$) and independently correlated with higher levels of VEGF ($P<.05$); there was no correlation between the expression of HIF-1α and the grade of the blood flow signal ($P>.05$). **Conclusion.** Ischemia-hypoxia conditions may be involved in the formation of MTrPs. CDFI can detect the features of angiogenesis in or surrounding MTrPs by assessing the blood flow signal.

The effect of ischemia – hypoxia in rats on angiogenesis in myofascial trigger points assessed by color Doppler flow imaging

Fangyan Jiang[1+], Shuangcheng Yu[2+], Haiqing Su[1], Shangyong Zhu[3*]

1 Department of Medical Ultrasound, the Affiliated Ethnic Hospital of Guangxi Medical University, No. 232, Ming Xiu Rd, 530001 Nanning, Guangxi, China;

2 Department of Radiology, the Affiliated Ethnic Hospital of Guangxi Medical University, No.232, Ming Xiu Rd., 530001 Nanning, Guangxi, China;

3 Department of Medical Ultrasound, the First Affiliated Hospital of Guangxi Medical University, No.6, Shuangyong Rd., 530021 Nanning, Guangxi, China.

*Corresponding Author:

Shangyong Zhu, No.6, Shuangyong Rd., 530021 Nanning, Guangxi, China. Email: zhushangyong2019@hotmail.com (S.Y.Z)

+Fangyan Jiang and Shuangcheng Yu contributed to this work equally.

Abstract

Background & Aims. Myofascial pain syndrome (MPS) is a common non-articular disorder of the musculoskeletal system which is characterized by the presence of myofascial trigger points (MTrPs). Despite the high prevalence of MPS, its pathogenesis, which induces the onset and maintenance of MTrPs, is still not fully understood. To date, there are no studies investigating the changes in the biochemical milieu with respect to ischemia and hypoxia that mentioned in the integrated hypothesis in the MTrPs region of the muscle. Therefore, this study was to investigate whether ischemia-hypoxic conditions are involved in the formation of MTrPs to affect angiogenesis assessed by color Doppler flow imaging (CDFI).

Methods. Twenty-five Sprague Dawley rats were randomly divided into a model group and a normal control group. The model of MTrPs was established by a blunt strike combined with eccentric exercise. Enzyme-linked immunosorbent assay (ELISA) analyses were employed to detect the serum levels of HIF-1α and VEGF. Microvessel density (MVD) was evaluated by immunohistochemistry. CDFI was applied to observe the blood flow signals in the MTrPs, which were graded as four types based on their strength.

Results. Compared with those in the control group, the expression of HIF-1α and VEGF as well as the MVD in the MTrPs group were significantly increased. This was accompanied by increased blood flow signals. In the MTrPs group, the grade of the blood flow signal was positively correlated with the MVD ($P < 0.05$) and independently correlated with higher levels of

VEGF ($P < 0.05$); there was no correlation between the expression of HIF-1α and the grade of the blood flow signal ($P > 0.05$).

Conclusion. Ischemia-hypoxia conditions may be involved in the formation of MTrPs. CDFI can detect the features of angiogenesis in or surrounding MTrPs by assessing the blood flow signal.

Keywords: Myofascial trigger points, Ischemia - hypoxic, Angiogenesis, Ultrasound, Color Doppler flow imaging

INTRODUCTION

Myofascial pain syndrome (MPS) is a common non-articular disorder of the musculoskeletal system affecting as many as 15% of patients in general medical practice and up to 85% in pain management centers (*Fleckenstein et al., 2010; Srbely et al., 2016*). MPS is characterized by the presence of MTrPs that are discrete, stiff and hyperirritable nodules in a palpable taut band of skeletal muscle during physical examination. Many physicians currently make a definite diagnosis of MPS by finding one or more MTrPs. Knowing the underlying etiology of MTrPs is critical not only to preventing their development and recurrence but also for inactivating and eliminating existing MTrPs (*Bron et al., 2012*). There is a consensus that muscle overuse, direct trauma or psychological stress are thought to lead to the development of MTrPs (*Simons et al., 1999*). Almost everyone has experienced muscle pain as a result of trauma, injury, overuse, or strain (*Shah et al., 2015*). If muscle pain persists long after the resolution of the injury factors, and normal recovery is disturbed, MTrPs may develop.

Despite the high prevalence of MPS, its pathogenesis, which induces the onset and maintenance of MTrPs, is still not fully understood (*Jafri et al., 2014*). At present, an intriguing possible mechanism mentioned by Simons, "The Integrated Trigger Point Hypothesis", is widely accepted by various researchers, which postulates that an "energy crisis" perpetuates an initial sustained low-level muscle contraction, and a decrease in intramuscular perfusion has been assumed (*Simons et al., 1999*). Thus, this leads to local ischemia, hypoxia, and insufficient ATP synthesis, which are responsible for increasing acidity and Ca2+ accumulation and subsequent sarcomere contracture. As long as sarcomere contracture persists, local intramuscular perfusion will be decreased, and ischemia and hypoxia will be increased. It is conceivable that the vicious cycle would likely lead to the development of MTrPs (*Shah et al., 2015; Simons et al., 1999*).

Previous studies have demonstrated that increased levels of pain and inflammatory biomarkers have been detected in the vicinity of active MTrPs (*Shah et al., 2008; Shah et al., 2005; Grosman-Rimon et al., 2016; Lv et al., 2018*). These findings objectively support Simons' integrated hypothesis. However, to date, there are no studies investigating the changes in the biochemical milieu with respect to ischemia and hypoxia in the MTrPs region of the muscle. It is not yet clear whether this phenomenon is involved in the progression of MTrPs. It is well known that hypoxia can enhance the expression of HIF-1α, which is an oxygen concentration-dependent key transcription factor, thereby regulating its downstream target gene VEGF (*Pugh et al., 2003*). This result has demonstrated the regulation of the process of angiogenesis under hypoxia – ischemia conditions (*Pugh et al., 2003*). In addition, VEGF is also confirmed to be involved in muscle repair mechanisms and skeletal muscle capillary formation, allowing the restoration of the blood flow to the injured tissue (*Olfert et al., 2010; Li et al., 2010*). Accordingly, it is likely that the levels of HIF-1α and VEGF increase in response to active MTrPs.

To this end, this study was conducted to establish an active MTrP model based on direct trauma in rats according to a previous study (*Huang et al., 2013*). The aim of the present study was to compare the levels of HIF-1α, VEGF and MVD between the active MTrP group and the normal control group to confirm hypoxia and ischemia, as mentioned in the integrated hypothesis, and to investigate whether these indicators are associated with the grades of the ultrasound blood flow signal.

MATERIALS AND METHODS

Experimental animals

Twenty-five healthy male Sprague Dawley rats that were 7 weeks old (body weight: 200–220 g) and purchased from the Animal Experiment Center of Guangxi Medical University (Nanning, China) were randomly divided into two groups: (1) normal control group (n = 10) and (2) model group (n = 15). All of the rats were kept in a pathogen-free animal facility with a controlled temperature of 22–24°C and 42% humidity， maintained under a constant 12 h dark/12 h light cycle. They were fed with free access to food and water. At the end of experiment, after obtaining the tissue section, all rats were euthanized through intraperitoneal injection of pentobarbital sodium (200 mg/kg). Animal experiments were conducted in accordance with local protocols for the care and use of laboratory animals. The procedures were all approved by the Animal Ethics Committee of Guangxi Medical University (Approval No: 201904013).

Animal model

The MTrP model was established as described by *Huang* et al (*Huang et al., 2013*) by a blunt strike combination with eccentric exercise for 8 weeks. The rats were anesthetized with an injection of 30 mg/kg pentobarbital sodium before being fixed on the board of a homemade striking device every Saturday. A blunt strike to the right proximal gastrocnemius, which had been marked on the skin, was performed by a 1200 g stick freely dropped from a height of 20 cm with a kinetic energy of 2.352 J (*Huang et al., 2013*). On the second day (every Sunday), all injured rats underwent 90-minute eccentric exercise on a treadmill (SA101B, Jiangsu Saiangsi Biological Technology Co., Ltd. Nanjing, China) at a −16° downhill angle and speed of 16 m/min (*Huang et al., 2013*). Subsequently, the rats rested for 5 days a week without any intervention. All rats in the model group were treated in this way for 8 weeks with a subsequent 4 weeks of rest, while the rats in the control group did not undergo any intervention in this period.

Ultrasound image Processing

After modeling, the fur and skin covering the right gastrocnemius area were shaved and cleaned. Then, all rats underwent an ultrasonographic examination using the Aplio 500 clinical ultrasound (US) system (Toshiba Medical System Corporation, Tokyo, Tochigi, Japan) with a linear array transducer (5–14 MHz). MTrPs were determined within the taut band by two diagnostic sonographers with 10 and 16 years of experience through a combination of grayscale imaging and sonoelastography. According to the previous literature (*Sikdar et al., 2009; Kumbhare et al., 2016; Shankar et al., 2012*), compared to the surrounding tissues, MTrPs are focal hypoechoic (darker) or hyperechoic (brighter) areas with heterogeneous echotextures on grayscale imaging and stiffer regions on sonoelastography. In the present study, strain elastography (SE) was

applied to identify the MTrPs through real-time color elastic graphs and grayscale US images. The hardness of tissues increased gradually as shown by the colors from green (soft tissue) to blue (hard tissue). CDFI was applied to detect blood flow in the MTrPs. The blood flow signals were semiquantitatively classified into four grades on the basis of the criteria of Adler (*Adler et al., 1990*): grade 0, no blood flow signal; grade I, one or two dot-like blood flow signals; grade II, three dot-like or thin and short blood flow signals; and grade III, one or more large and long blood flow signals (Fig. 1).

In cases of the presence of more than one MTrP diagnosed by US imaging within the gastrocnemius area, the point with the richest blood flow signal in the referenced location was chosen.

Electromyographic and histological assays

The examination of all rats was performed by an electromyographic (EMG) device (NTS-2000, Nuocheng Medical Co., Ltd., Shanghai) to record the EMG. First, the right gastrocnemius area of rats was completely exposed. The palpable taut band of muscle was marked. Then, the electrode was inserted into the taut bands to detect the spontaneous electrical activity (SEA), which determined the presence of active MTrPs (*Huang et al., 2013*). After the SEA was determined, segments of corresponding tissue in muscle were cut off and fixed in formalin buffer to subsequently reveal the histological changes of active MTrPs. Similarly, rats in the control group underwent EMG, and histological assays were performed at the same positions.

148 **Microvessel density analysis**

149 MVD of the gastrocnemius muscles of rats from the two groups was detected by hematoxylin-
150 eosin (HE) staining. Paraffin sections were fixed and stained with HE. The primary anti-CD31
151 antibody (1: 500, v/v) used to detect vascular endothelial cells was added and incubated
152 overnight at 4°C. After three 5-min washes, the secondary anti-mouse IgG (1:2000) antibody
153 was incubated at 37°C for 1 h. Then, the samples were washed with PBS buffer. The hotspot
154 method was applied to determine the MVD as previously proposed by Weidner (*Weidner et al.,*
155 *1991*)**.** Three areas of increased vascularization were selected under a 40 x optical field of view.
156 The average microvessel counts in three selected fields were calculated under 200 x
157 magnification.

158

159 **Enzyme-linked immunosorbent assay analysis**

160 Due to the extremely small size of MTrPs (3-4 mm^2), muscle tissues were obtained from the
161 vicinity of MTrPs and stored at -80°C to increase the sensitivity of the test sample. Tissue
162 samples (100 mg) were homogenized at 4°C and centrifuged for 5 min at 5000 rpm and 2 - 8°C.
163 ELISA was utilized to quantify the concentrations of HIF-1α and VEGF by strictly following the
164 manufacturer's instructions (Cusabio Biotech CO., Ltd., Wuhan, China).

165

166 **Statistical analysis**

167 All data were analyzed with SPSS 22.0 software (Chicago, IL, USA). The data normality was
168 checked by the Komogorov-Sminorv test. Descriptive statistics including the levels of HIF-1α

and VEGF and the results of MVD are presented as the mean and standard deviation. The Independent-Samples T Test was used to verify the differences between the MTrP group and the normal control group. The correlations between the grade of the blood flow signal, MVD, VEGF and HIF-1α were calculated using the Spearman rank correlation coefficient. For all tests used, statistical significance was set at a value of $P < .05$.

RESULTS

Of the 15 modeling rats, one died unexpectedly due to anesthesia. Therefore, a total of 24 rats survived in the present study (model group: n = 14, normal group: n = 10).

Ultrasound findings

In B-mode imaging, MTrPs were visualized in all rats of the model group within the taut band of the right gastrocnemius muscle, which was consistent with the location of the palpable nodule during physical examination, while no MTrPs were found in the control group. The great majority of MTrPs showed an ellipsoidal, focal, hypoechoic region, and 2 rats exhibited a hyperechoic region. Among them, 4 rats had more than one hypoechoic region, and the point of the greatest blood flow signal was chosen. The average size of MTrPs was 3.3 ± 0.18 mm^2. In addition, SE imaging consistently detected a focal stiff region that was entirely covered in blue or mostly blue with little green. These findings were in agreement with what has been described by Kumbhare et al (*Kumbhare et al., 2016*). (Fig. 2).

188 CDFI examination indicated that the vessels in and around MTrPs were richer than the
189 normal muscle tissue, which showed no blood flow signal. The detailed data for the rats from the
190 MTrP group are listed in Table 1.

191

192 **EMG and pathological features**

193 The taut bands of the muscles presenting with abnormal ultrasonic changes were verified to show
194 spontaneous electrical activities and local twitch responses by an EMG device. The rats in the
195 normal control group showed no EMG activity (Fig. 3).

196 The pathological sections from the area of MTrPs revealed that muscle fibers varied in shape
197 and size. Specifically, muscle fibers became thinner at both ends and swelled in the middle with
198 contraction nodules in the longitudinal section and local muscle fiber gap widening. However,
199 the size and shape of muscle fibers from normal controls were uniform (Fig. 4). This was
200 consistent with what has been noted in the previous literature (*Zhang et al., 2017*).

201

202 **MVD detection**

203 As shown in Fig. 5, the cytoplasm of vascular endothelial cells in the gastrocnemius muscles of
204 rats was stained brownish-yellow by labelling of CD31 protein. The MVD of the model and
205 control groups under 200 x optical magnification were 123.64±9.56 and 84.70±13.46,
206 respectively. The MVD of the MTrP group was significantly higher than that of the control
207 group ($p = .000$). Additionally, by comparing the vascular morphology of the two groups, it was

found that the blood vessels in the MTrP group were thicker and less regularly distributed than those in the control group.

Expression of HIF-1α and VEGF in the two groups

To investigate ischemia and hypoxia in the MTrPs, the serum levels of HIF-1α and its downstream target gene VEGF were detected by ELISA. As displayed in Fig. 6, the expression of HIF-1α and VEGF in the MTrP group was significantly higher than that in the normal control group ($p < .05$).

Correlation analysis of HIF-1α, VEGF and MVD with blood flow signals in the MTrP group

In the MTrP group, the serum levels of VEGF and MVD were positively correlated with the grades of the blood flow signal, and the correlation coefficients were 0.595 and 0.761, respectively. There was no significant association between the levels of HIF-1α and the grades of the blood flow signal (Table 2).

DISCUSSION

The present study was undertaken to determine whether ischemia–hypoxia, as mentioned in the integrated hypothesis, is involved in the formation of MTrPs and the underlying effect on angiogenesis. The preliminary findings in this study demonstrate that (1) significantly increased

levels of HIF-1α and VEGF as well as an increase in the MVD in rats with MTrPs compared with those in the normal controls; (2) the grade of blood flow signals detected by CDFI was positively correlated with VEGF expression and the MVD. These results were in line with the intramuscular changes associated with the ischemia–hypoxia microenvironment, suggesting an objective basis of support for the integrated hypothesis of MTrPs.

As expected in the present study, the active MTrP rat model was successfully established by a blunt strike combined with eccentric exercise, which was confirmed through changes in palpation, US imaging, local twitch response, EMG and pathology according to the criteria defined by Travel and Simons (*Simons et al., 1999*). Eccentric exercise can result in muscle pain and damage because muscle fibers are stretched irregularly and unevenly to a point beyond the filament overlap（*Gerwin et al., 2004*）. Based on eccentric exercise, the right gastrocnemius muscle was struck, which was different from the left medial femoral muscle, as suggested by another study (*Huang et al., 2013*), because the gastrocnemius muscle is always clinically involved in chronic myofascial pain(*Benito-de-Pedro et al., 2020*). Previous studies have shown that eccentric exercise in rats or mice produced more damage in the gastrocnemius than in the tibialis anterior muscle, which was attributed to the flexor muscle undergoing longer eccentric exercise than the dorsiflexor during downhill running (*Marqueste et al., 2008; Mathur et al., 2011*).

Increased levels of HIF-1α and VEGF were detected in the MTrP group, which was consistent the major role of hypoxia in the overall process (*Pugh et al., 2003*). Previous studies have demonstrated that HIF-α levels are generally low in normal hypoxic rodent tissues and may not be detectable even in areas of physiological hypoxia, such as the renal medulla (*Pugh et al., 2003;*

250 *Rosenberger et al., 2002*). When systemic hypoxia or tissue ischemia increases, HIF-α levels are
251 enhanced and subsequently induce the expression of VEGF (*Pugh et al., 2003*). Ischemia and
252 hypoxia are usually followed by the stimulation of tissue angiogenesis. Blood vessel formation is
253 linked to growth factors. However, the great majority of data on angiogenesis came from
254 pathophysiological studies of vasculature and tumors (*Tamura et al., 2019*) . In fact, other studies
255 have shown that the induction of HIF-1α can be activated under a range of ischemic, hypoxic and
256 inflammatory conditions, such as wounding of skin (*Elson et al., 2000*) , arthritis (*Feng et al.,*
257 *2019*), and colonic inflammation (*Wang et al., 2017*). Similarly, the present data from the MTrP
258 group also demonstrated an obvious increase in the MVD compared to that in the normal control,
259 suggesting that angiogenesis was promoted in zones of MTrPs. This finding was in agreement
260 with a report that revealed VEGF as a growth factor involved in skeletal muscle repair
261 mechanisms and capillary formation (*Grosman-Rimon et al., 2016*).

262 The ischemia and hypoxia at the trigger point may be closely associated with sustained
263 contraction of muscles to shape local hypercontractions, which result in high intramuscular
264 pressure to compress capillaries and impede local muscle blood flow, a condition that would lead
265 to intramuscular hypoperfusion and local ischemia (*Gerwin et al., 2004; Sikdar et al., 2010*).
266 Hypoxia is involved in MTrPs, which is in line with the concept of circulation hypoperfusion
267 because ischemia generates hypoxia (*Gerwin et al., 2004*). Due to continuous ischemia and
268 hypoxia, low levels of adenosine triphosphate (ATP) and mitochondrial dysfunction are likely to
269 occur and form a vicious cycle, resulting in an ischemia-induced energy crisis in myofascial
270 syndromes (*Simons et al., 1999; Gerwin et al., 2004*).

271 Although the diagnosis of MTrPs was determined by conventional US combined with SE
272 examination, the aim of this study was to investigate the features of blood flow signals. To date,

only three studies (*Sikdar et al., 2009;Sikdar et al., 2010; Ballyns et al., 2011*) have attempted to characterize the features of the Doppler flow waveform to examine the highly resistive vascular bed in and around the MTrPs. There were no studies to assess the characteristics of angiogenesis at a trigger point. CDFI is the most common tool used to sensitively visualize blood flow. The data of this study revealed that the signals of blood flow were stronger in the MTrP group than in the control group. Conspicuous blood vessels were found at 12 of the 14 sites in the MTrP group, while no blood flow signals were found in the controls. Intriguingly, the signals of blood flow in the zone of MTrPs were mainly at level I-II (9 / 14), with 3 cases at level III, suggesting that the majority of subjects presented with dot-like or short blood flow signals. Two cases were found in which a large and long blood vessel passed through the trigger point, as previously reported (*Sikdar et al., 2010*).

In addition, the grades of blood flow signals were positively correlated with VEGF expression and the MVD in the MTrP group. The correlation with VEGF was weaker than that with the MVD. There were three possible factors explaining this weak correlation. First, the MVD is not only proposed as a standard indicator to determine the number of angiogenesis events (*Magnon et al., 2007*) but also to intuitively reflect the morphology and distributive features of microvessels. Correspondingly, our findings demonstrated that the neovascularization of MTrPs was increased compared to that in normal muscles; blood vessel formation, expansion and irregular distribution were also observed in the MTrPs, which obviously differed from the uniform and regular distribution of blood vessels in controls. Second, VEGF is just one of the factors that promotes angiogenesis, and other growth factors, such as fibroblast growth factor-2 (FGF-2) and platelet-derived growth factor (PDGF), are also important (*Grosman-Rimon ., 2016*). VEGF studies may be relatively more common in the literature than other studies. VEGF

296 expression is generally shown to closely correlate with the MVD (*Zou et al., 2016; Maria et al.,*
297 *2005*). Third, there may be a time interval between VEGF expression in the MTrPs and the
298 subsequent blood vessel formation detectable by CDFI.

299 This study had some limitations. First, both hypoechoic and hyperechoic regions were imaged in
300 the present study, and their special structures in the taut bands were not investigated. Second,
301 although the feasibility of using strain elastography to aid in the identification of MTrPs has been
302 demonstrated, standardization of the imaging procedure was not further analyzed. Although this
303 initial work has shown a significant difference between MTrPs and normal controls in terms of
304 the presence of blood flow signals, there is much room for the improvement of the identification
305 of MTrPs on US imaging. More research to morphologically visualize MTrPs to determine their
306 differences from surrounding tissue is needed.

307

308 **CONCULSION**

309 The present study demonstrates that the levels of HIF-1α and VEGF as well as the MVD were
310 significantly higher in the MTrP group than those in the normal controls, indicating that these
311 are affected by muscle ischemia - hypoxia. These findings support that ischemia-hypoxia is
312 involved in the formation of MTrPs. In addition, it was also shown that the grades of the blood
313 flow signals were positively correlated with the expression of VEGF and the MVD in the MTrP
314 group, suggesting that CDFI is able to detect the features of angiogenesis in or surrounding
315 MTrPs by assessing the signals of blood flow.

316

Acknowledgments

The authors thank the Animal experiment center of GuangXi Medical University for the animal rooms and technical assistance.

REFERENCES

Fleckenstein J, Zaps D, Ruger LJ et al. 2010. Discrepancy between prevalence and perceived effectiveness of treatment methods in myofascial pain syndrome: results of a cross-sectional, nationwide survey. BMC Musculoskelet Disord **11**;11:32 DOI 10.1186/1471-2474-11-32.

Srbely JZ, Kumbhare D, Grosman-Rimon L.2016. A narrative review of new trends in the diagnosis of myofascial trigger points: diagnostic ultrasound imaging and biomarkers. J Can Chiropr Assoc **60(3):**220-225 PMID: 27713577.

Bron C, Dommerholt JD. 2012. Etiology of Myofascial Trigger Points. Current Pain and Headache Reports **16**:439–444 DOI 10.1007/s11916-012-0289-4.

Shah JP, Thaker N, Heimur J, Aredo JV, Sikdar S, Gerber L. 2015. Myofascial Trigger Points Then and Now: A Historical and Scientific Perspective. PM R**7(7)**:746-761 DOI 10.1016/j.pmrj.2015.01.024.

Jafri SM. 2014. Mechanisms of Myofascial Pain. International Scholarly Research Notices. DOI 10.1155/2014/523924.

Simons DG, Travell JG, Simons LS. 1999. Travell and Simons´myofascial pain and dysfunction: the trigger point manual. Volume 1: upper half of body, 2nd ed. Baltimore: Williams Wilkins 71-72. DOI：10.1097/00008506-200101000-00026.

Shah JP, Danoff JV, Desai MJ, Parikh S, Nakamura LK, Phillips TM, Gerber LH. 2008. Biochemicals associated with pain and inflammation are elevated in sites near to and remote from active myofascial trigger points. Arch Phys Med Rehabil **89**:16–23 DOI 10.1016/j.apmr.2007.10.018.

Shah JP, Phillips TM, Danoff JV, Gerber LH. 2005. An in vivo microanalytical technique for measuring the local biochemical milieu of human skeletal muscle. J Appl Physiol (Bethesda, Md: 1985) **99**:1977–84 DOI 10.1152/japplphysiol.00419.2005

Grosman-Rimon L, Parkinson W, Upadhye S, Clarke H, Katz J, Flannery J, Peng P, Kumbhare D. 2016. Circulating biomarkers in acute myofascial pain: A case-control study. Medicine **95**(37):e4650 DOI 10.1097/MD.0000000000004650.

Lv H, Li Z, Hu T, Wang Y, Wu J, Li Y. 2018. The shear wave elastic modulus and the increased nuclear factor kappa B (NF-kB/p65) and cyclooxygenase-2 (COX-2) expression in the area of myofascial trigger points activated in a rat model by blunt trauma to the vastus medialis. J Biomech **3**;66:44-50 DOI 10.1016/j.jbiomech.2017.10.028.

356 **Pugh CW, Ratcliffe PJ. 2003.** Regulation of angiogenesis by hypoxia: Role of the HIF system.
357 Nat Med **9**: 677-684 DOI 10.1038/nm0603-677

358 **Olfert IM, Howlett RA, Wagner PD, Breen EC. 2010.** Myocyte vascular endothelial growth
359 factor is required for exercise-induced skeletal muscle angiogenesis. Am J Physiol Regul
360 Integr Comp Physiol **299**:R1059–67 DOI 10.1152/ajpregu.00347.2010.

361 **Li J, Wei Y, Liu K, Yuan C, Tang YJ, Quan QL, Chen P, Wang W, Hu HZ, Yang L. 2010.**
362 Synergistic effects of FGF-2 and PDGF-BB on angiogenesis and muscle regeneration in
363 rabbit hindlimb ischemia model. Microvasc Res **80**:10–7 DOI
364 10.1016/j.mvr.2009.12.002.

365 **Huang Q, Ye G, Zhao Z, Lv J, Tang L. 2013.** Myoelectrical activity and muscle morphology
366 in a rat model of myofascial trigger points induced by blunt trauma to the vastus medialis.
367 Acupunct Med **31**, 65–73 DOI 10.1136/acupmed-2012-010129.

368 **Sikdar S, Shah JP, Gebreab T, Yen RH, Gilliams E, Danoff J, Gerber LH. 2009.** Novel
369 Applications of ultrasound technology to visualize and characterize myofascial trigger
370 points and surrounding soft tissue. Arch Phys Med Rehabil **90**:1829-38
371 DOI 10.1016/j.apmr.2009.04.015.

372 **Kumbhare DA, Elzibak AH, Noseworthy MD. 2016.** Assessment of Myofascial Trigger Points
373 Using Ultrasound. Am J Phys Med Rehabil **95**(1):72-80
374 DOI 10.1097/PHM.0000000000000376.

375 **Shankar H, Reddy S. 2012.** Two- and three-dimensional ultrasound imaging to facilitate
376 detection and targeting of taut bands in myofascial pain syndrome. Pain Med **13**:971- 5
377 DOI 10.1111/j.1526-4637.2012.01411.x.

378 **Adler DD, Carson PL, Rubin JM, Quinn-Reid D. 1990.** Doppler ultrasound color flow
379 imaging in the study of breast cancer; Preliminary findings. Ultrasound Med Biol **16**:553-
380 559
381 DOI 10.1016/0301-5629(90)90020-d.

382 **Weidner N,Semple JP, Welch WR, Folkman J. 1991.** Tumor angiogenesis and metastasis-
383 correlation in invasive breast carcinoma. N Engl J Med **324**:1-8
384 DOI: 10.1056/NEJM199101033240101.

385 **Zhang H, Lü J, Huang Q, Liu L, Liu Q, Eric O. 2017.** Histopathological nature of myofascial
386 trigger points at different stages of recovery from injury in a rat model. Acupunct Med
387 **35(6)**:445-451 DOI 10.1136/acupmed-2016-011212.

388 **Gerwin RD, Dommerholt J, Shah JP. 2004.** An expansion of Simons' integrated hypothesis of
389 trigger point formation. Curr Pain Headache Rep **8**:468–475 DOI 10.1007/s11916-004-
390 0069-x.

391 **Benito-de-Pedro M, Becerro-de-Bengoa-Vallejo R, Elena Losa-Iglesias M, Rodríguez-Sanz**
392 **D , López-López D , Palomo-López P , Mazoteras-Pardo V, César Calvo-Lobo A.**
393 **2020.** Effectiveness of Deep Dry Needling vs Ischemic Compression in the Latent
394 Myofascial Trigger Points of the Shortened Triceps Surae from Triathletes on Ankle

Dorsiflexion, Dynamic, and Static Plantar Pressure Distribution: A Clinical Trial. Pain Med **21(2)**: e172-e181 DOI 10.1093/pm/pnz222.

Marqueste T, Giannesini B, Fur YL, Cozzone PJ, Bendahan D. 2008. Comparative MRI analysis of T2 changes associated with single and repeated bouts of downhill running leading to eccentric-induced muscle damage. J Appl Physiol **105**:299-307 DOI 10.1152/japplphysiol.00738.2007

Mathur S, Vohra RS, Germain SA, Forbes S, Bryant ND, Vandenborne K, Walter AG. 2011. Changes in muscle T2 and tissue damage after downhill running in mdx mice. Muscle Nerve **43(6)**:878-86 DOI 10.1002/mus.21986.

Rosenberger, C, Mandriota S, Jürgensen JS, Wiesener MS, Hörstrup JH, Frei U, Ratcliffe PJ, Maxwell PH, Bachmann S, Eckardt KU. 2002. Expression of hypoxia-inducible factor-1α and -2α in hypoxic and ischemic rat kidneys. J. Am. Soc. Nephrol **13**: 1721–1732 DOI 10.1097/01.asn.0000017223.49823.2a.

Tamura R, Tanaka T, Akasaki Y, Murayama Y, Yoshida K, Sasaki H. 2019. The role of vascular endothelial growth factor in the hypoxic and immunosuppressive tumor microenvironment: perspectives for therapeutic implications. Med Oncol **37**(1):2 DOI 10.1007/s12032-019-1329-2.

Elson DA, Ryan HE, Snow JW, Johnson, Arbeit JM. 2000. Coordinate up-regulation of hypoxia inducible factor (HIF)-1α and HIF-1 target genes during multistage epidermal carcinogenesis and wound healing. Cancer Res **60**:6189–6195 DOI：

10.1046/j.1523-5394.2000.86004.x

Feng Z, Yang T, Hou X, Wu H, Feng J, Ou B, Cai SJ, Li J, Mei ZH. 2019. Sinomenine mitigates collagen-induced arthritis mice by inhibiting angiogenesis. Biomed Pharmacother. **113**:108759 DOI 10.1016/j.biopha.2019.108759.

Wang S, Tao P, Hu H, Yuan J, Zhao L, Sun B, Zhang WJ, Li J. 2017. Effects of initiating time and dosage of Panax notoginseng on mucosal microvascular injury in experimental colitis. World J Gastroenterol **23**(47):8308-8320 DOI 10.3748/wjg.v23.i47.8308.

Sikdar S, Ortiz R, Gabreab T, Gerber LH, Shah JP. 2010. Understanding the vascular environment of myofascial trigger points using ultrasonic imaging and computational modeling. Conf Proc IEEE Eng Med Biol Soc 5302-5

DOI 10.1109/IEMBS.2010.5626326

Ballyns JJ, Shah JP, Hammond J, Gebreab T, Gerber LH, Sikdar S. 2011. Objective sonographic measures for characterizing myofascial trigger points associated with cervical pain. J Ultrasound Med **30**（10）: 133 1- 1340 DOI 10.7863/jum.2011.30.10.1331.

Magnon C, Galaup A, Rouffiac V, Opolon P, Connault E, Rosé M, Perricaudet M, Roche A, Germain S, Griscelli F, Lassau N. 2007. Dynamic assessment of antiangiogenic therapy by monitoring both tumoral vascularization and tissue degeneration. Gene Ther **14**:108-117 DOI 10.1038/sj.gt.3302849.

Raspollini MR,Castiglione F, Garbini F, Villanucci A, Amunni G, Baroni G, Boddi V, Taddei GL. 2005. Microdensity vessels and with vascular endothelial growth factor expression in ovarian carcinoma. Int J Surg Pathol **13**:135-142

436 DOI 10.1177/106689690501300202.

Figure 1

Description of different grades of blood flow signals in the MTrPs on color Doppler flow imaging

(A) grade 0, no blood flow signals; (B) grade I, one or two dot-like blood flow signals; (C) grade II, three dot-like or thin and short blood flow signals; (D) grade III, one or more large and long blood flow signals.

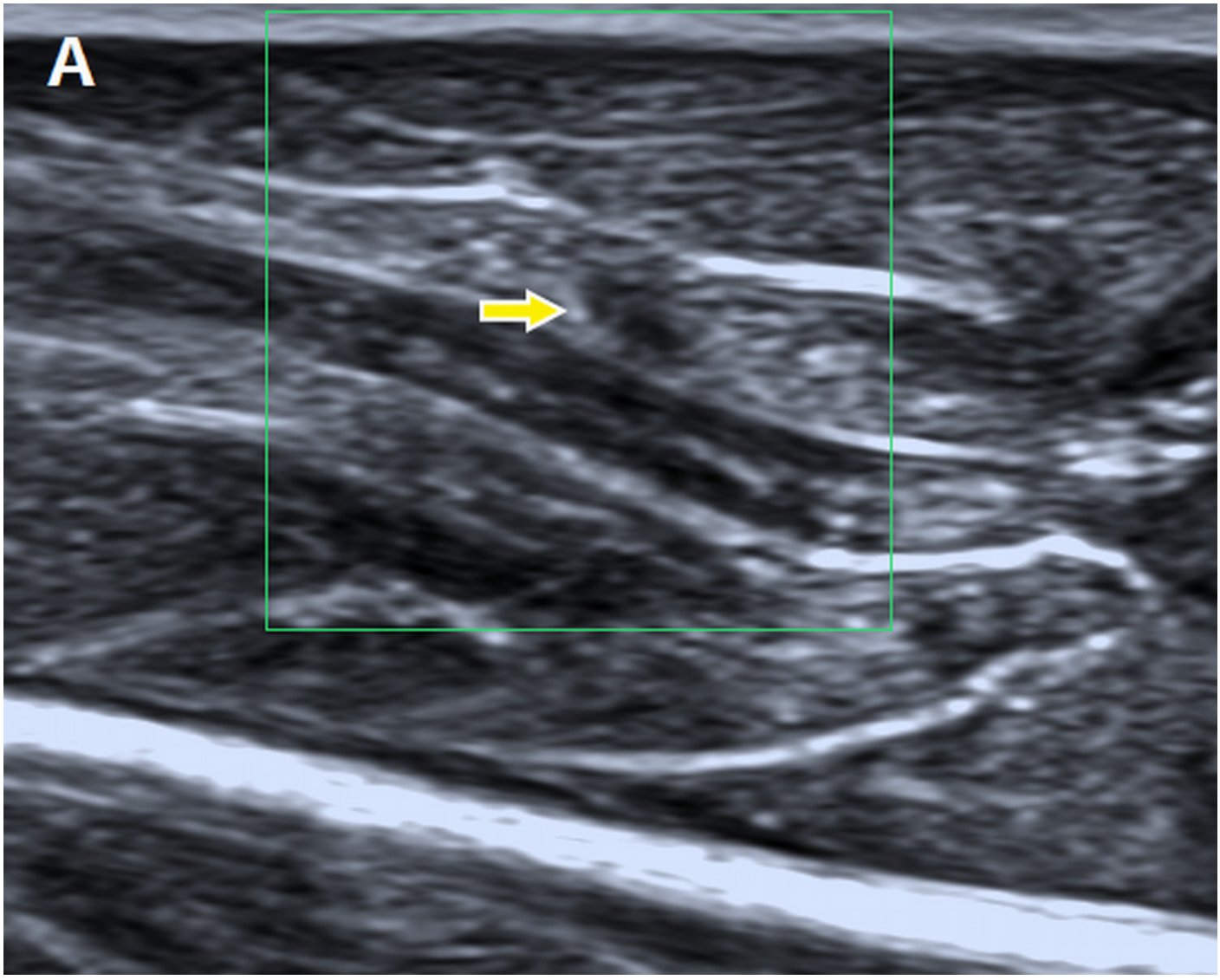

Figure 2

Description of different grades of blood flow signals in the MTrPs on color Doppler flow imaging

（A）grade 0, no blood flow signals; （B）grade I, one or two dot-like blood flow signals; （C）grade II, three dot-like or thin and short blood flow signals; （D）grade III, one or more large and long blood flow signals.

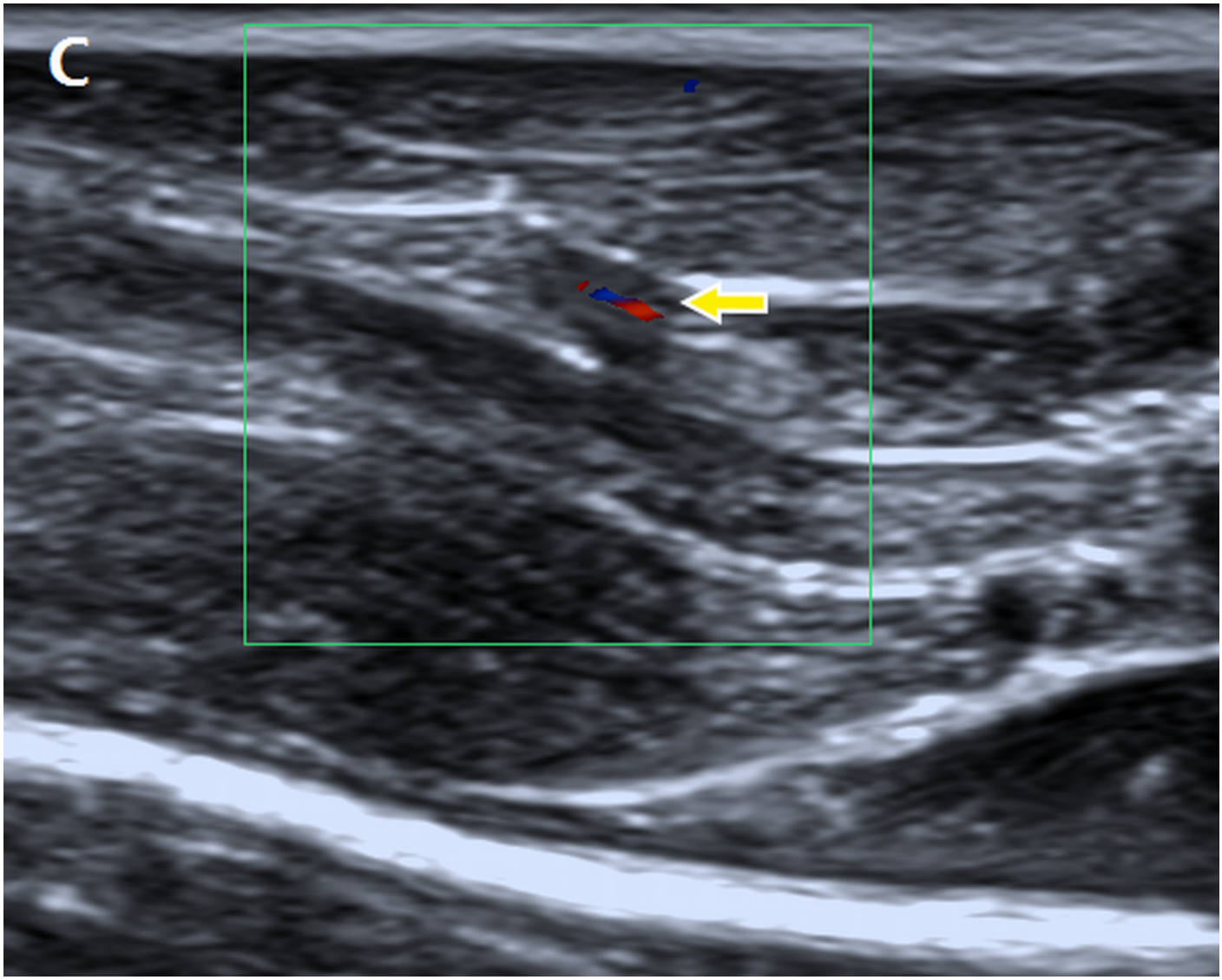

Figure 3

Description of different grades of blood flow signals in the MTrPs on color Doppler flow imaging

(A) grade 0, no blood flow signals; (B) grade I, one or two dot-like blood flow signals; (C) grade II, three dot-like or thin and short blood flow signals; (D) grade III, one or more large and long blood flow signals.

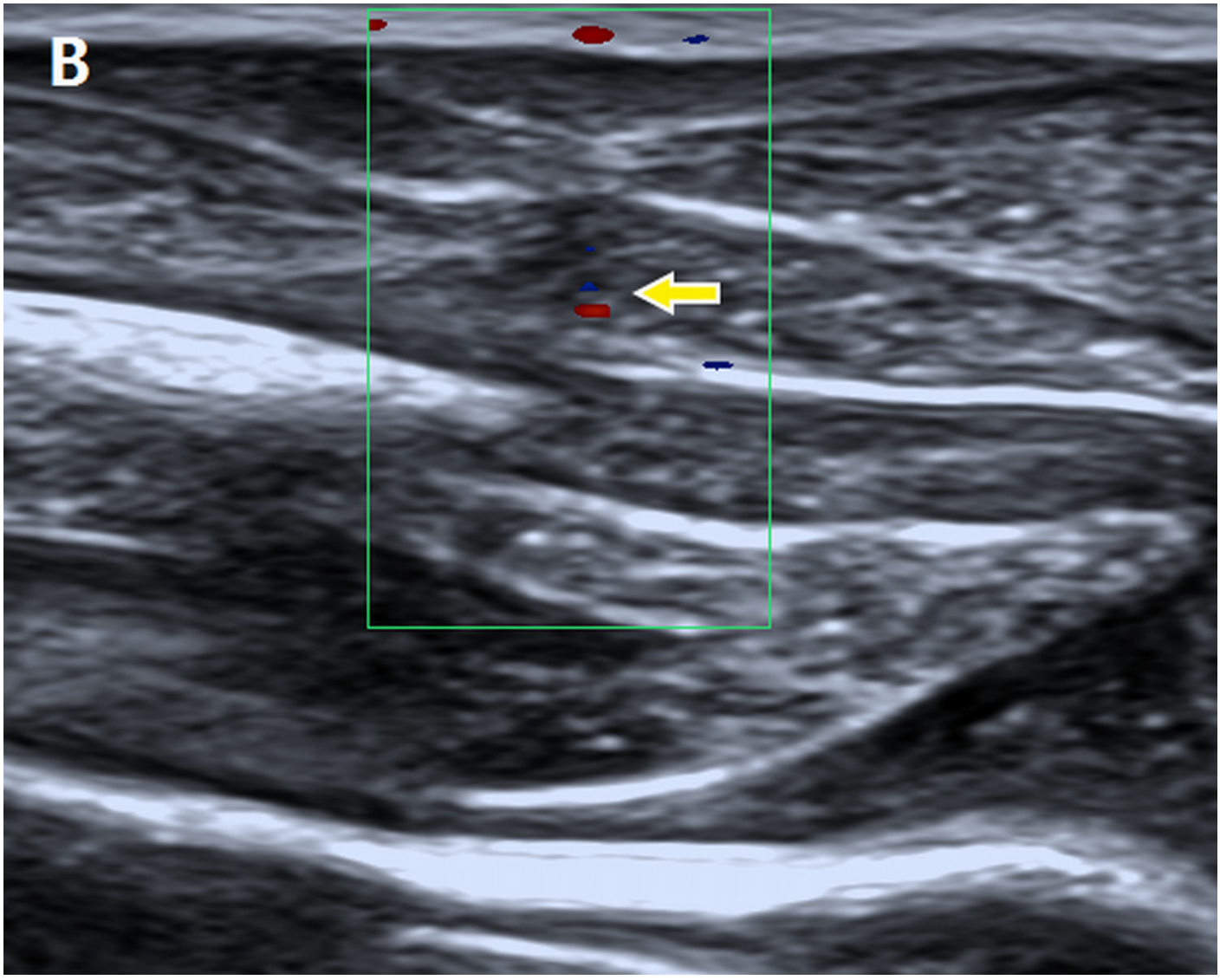

Figure 4

Description of different grades of blood flow signals in the MTrPs on color Doppler flow imaging

(A) grade 0, no blood flow signals; (B) grade I, one or two dot-like blood flow signals; (C) grade II, three dot-like or thin and short blood flow signals; (D) grade III, one or more large and long blood flow signals.

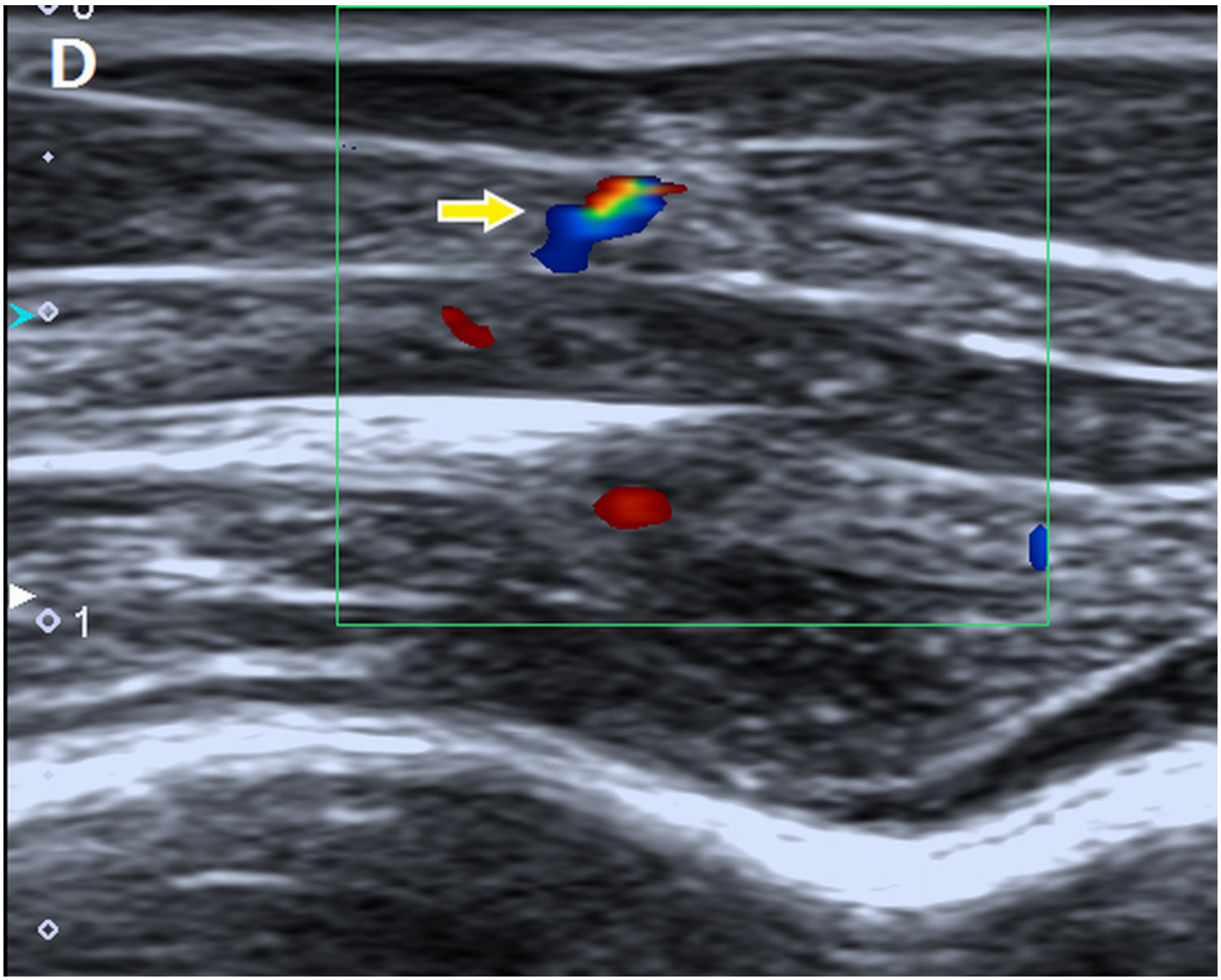

Figure 5

The screenshot of the sonoelastography modes. Strain elastography detection of a focal stiff region

(A) and (B) entirely covered in blue or mostly blue with little green compared to the adjacent normal muscle tissue.

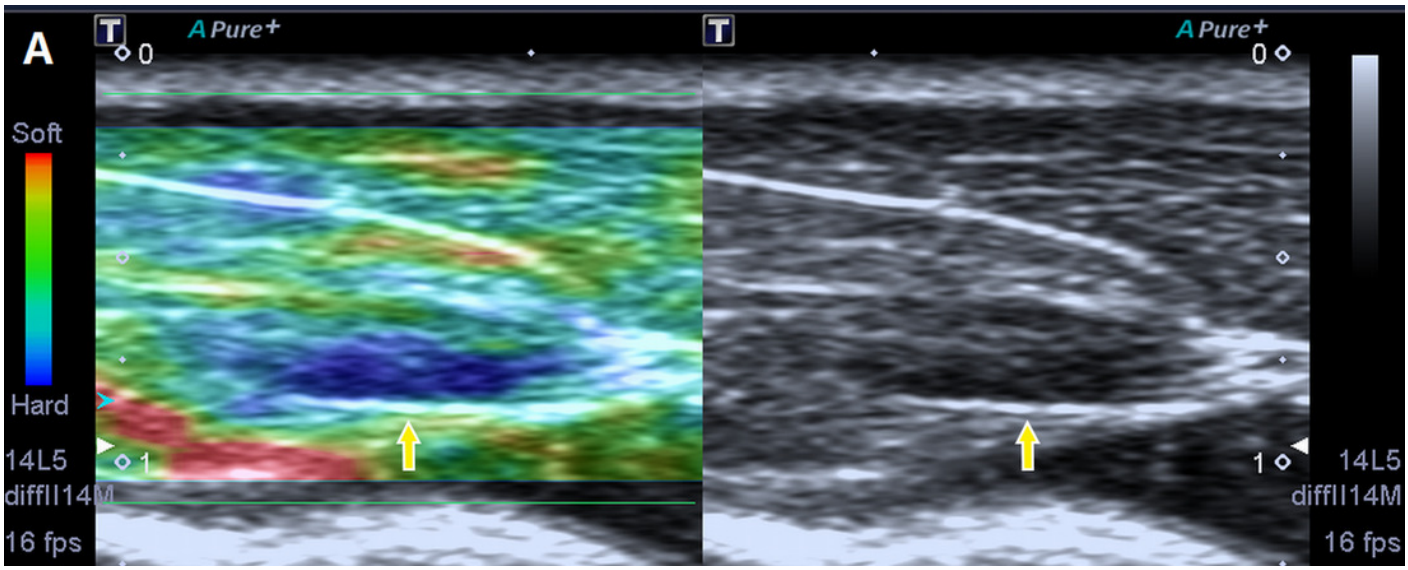

Figure 6

The screenshot of the sonoelastography modes. Strain elastography detection of a focal stiff region

(A) and (B) entirely covered in blue or mostly blue with little green compared to the adjacent normal muscle tissue.

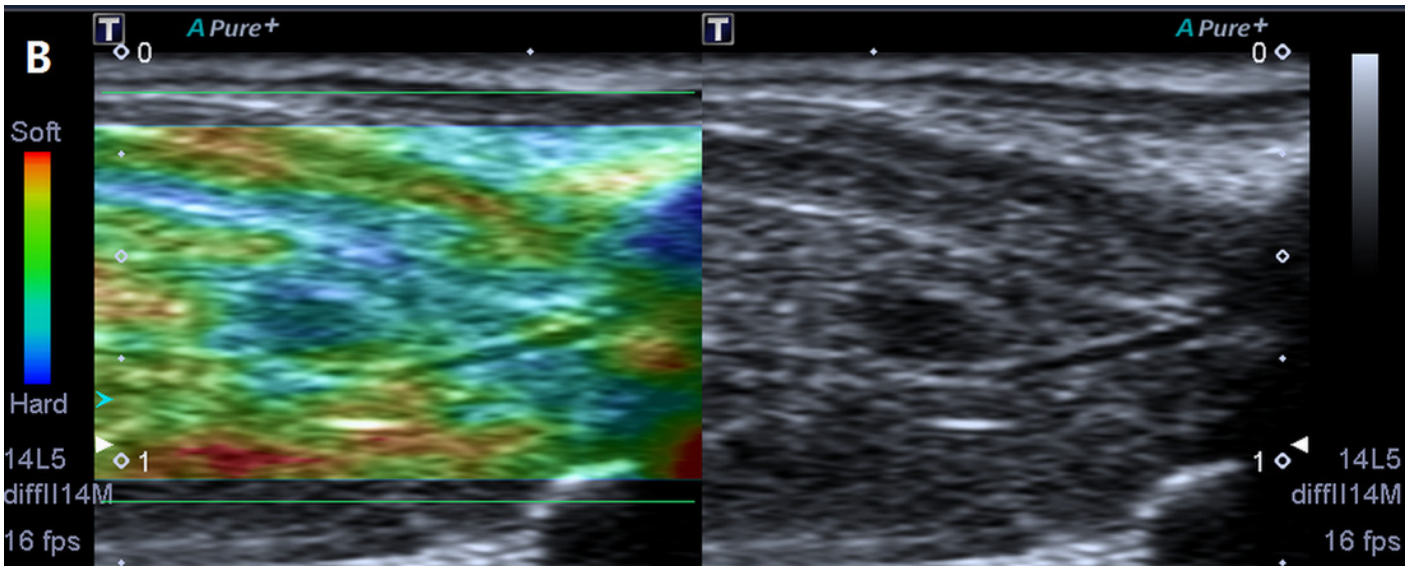

Figure 7

Electromyography (EMG) recordings from two groups

(A) muscle fibres from MTrPs presenting with spontaneous electrical activities; (B) muscle fibres from normal controls showing no EMG activity.

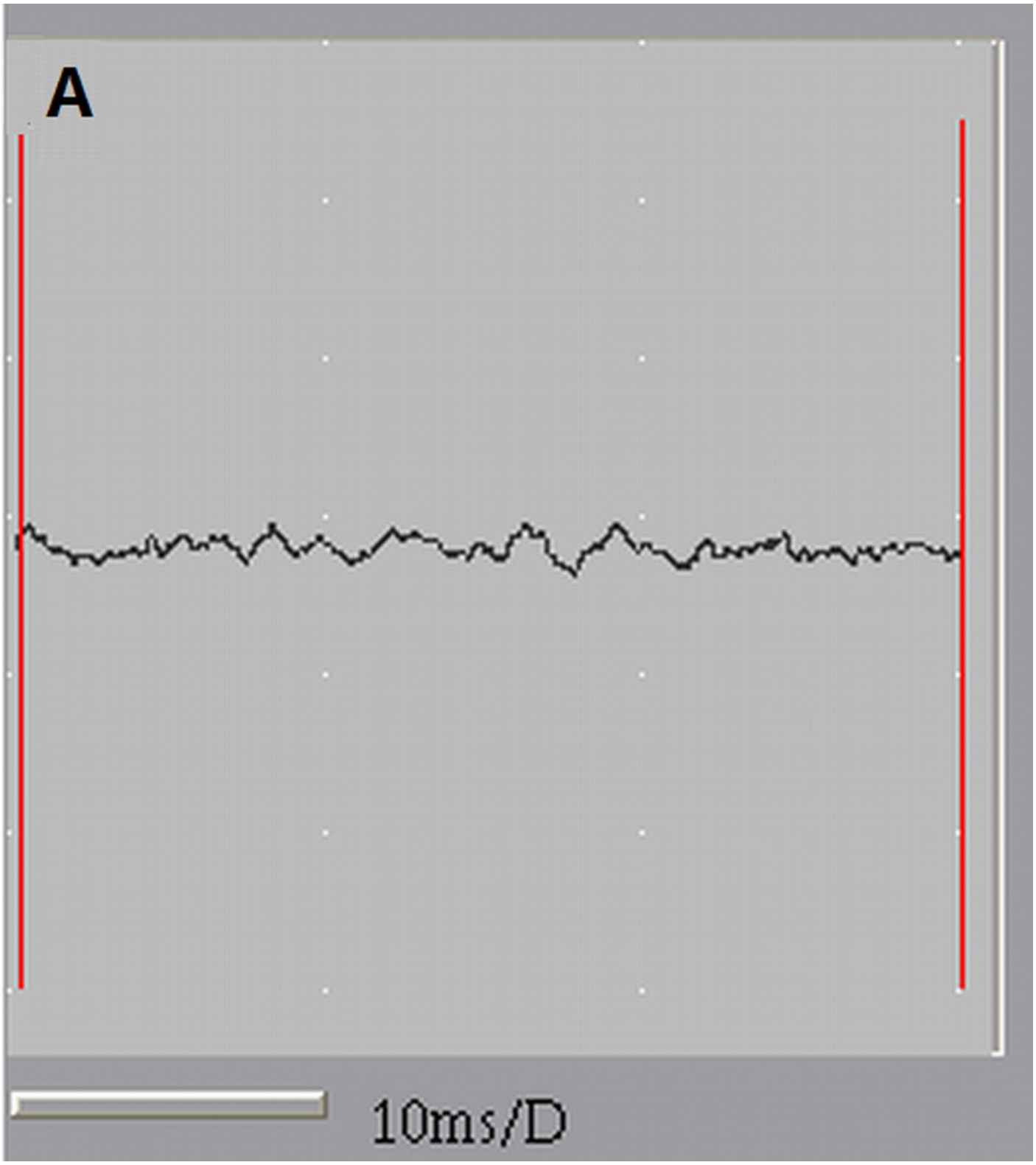
A
10ms/D

Figure 8

Electromyography (EMG) recordings from two groups

(A) muscle fibres from MTrPs presenting with spontaneous electrical activities; (B) muscle fibres from normal controls showing no EMG activity.

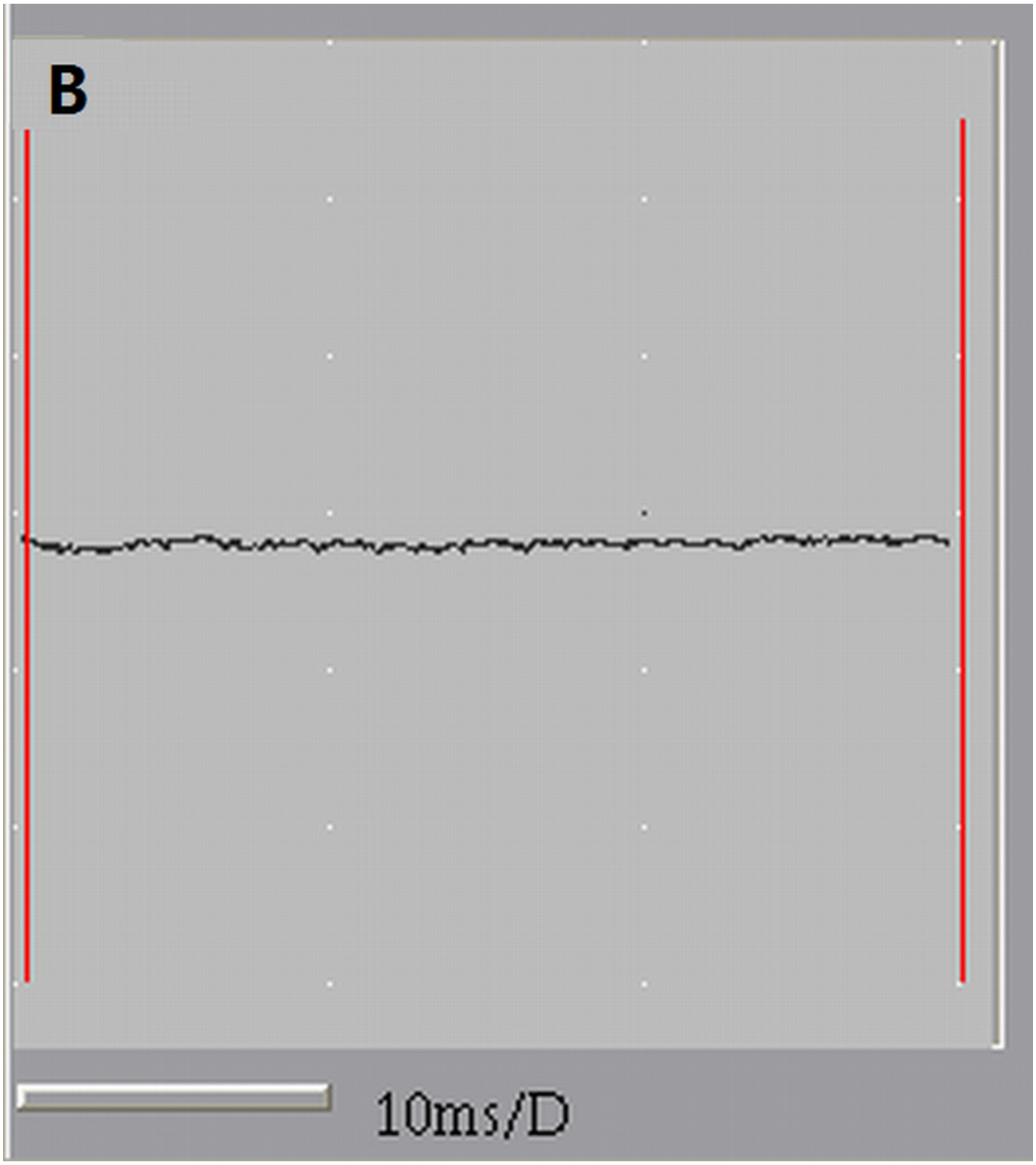
B
10ms/D

Figure 9

Microscopic views of muscle fibers from two groups of rats with HE staining (400×)

The histological changes of MTrPs are depicted in (A) (cross-section) and (B)(longitudinal section), which show that muscle fibers became thinner at both ends and swelled in the middle to show the contraction nodules in longitudinal section along with local muscle fiber gap widening. The histologically normal muscle fibers are similarly shown in (C) and (D), which reveal that the size and shape of muscle fibers are uniform.

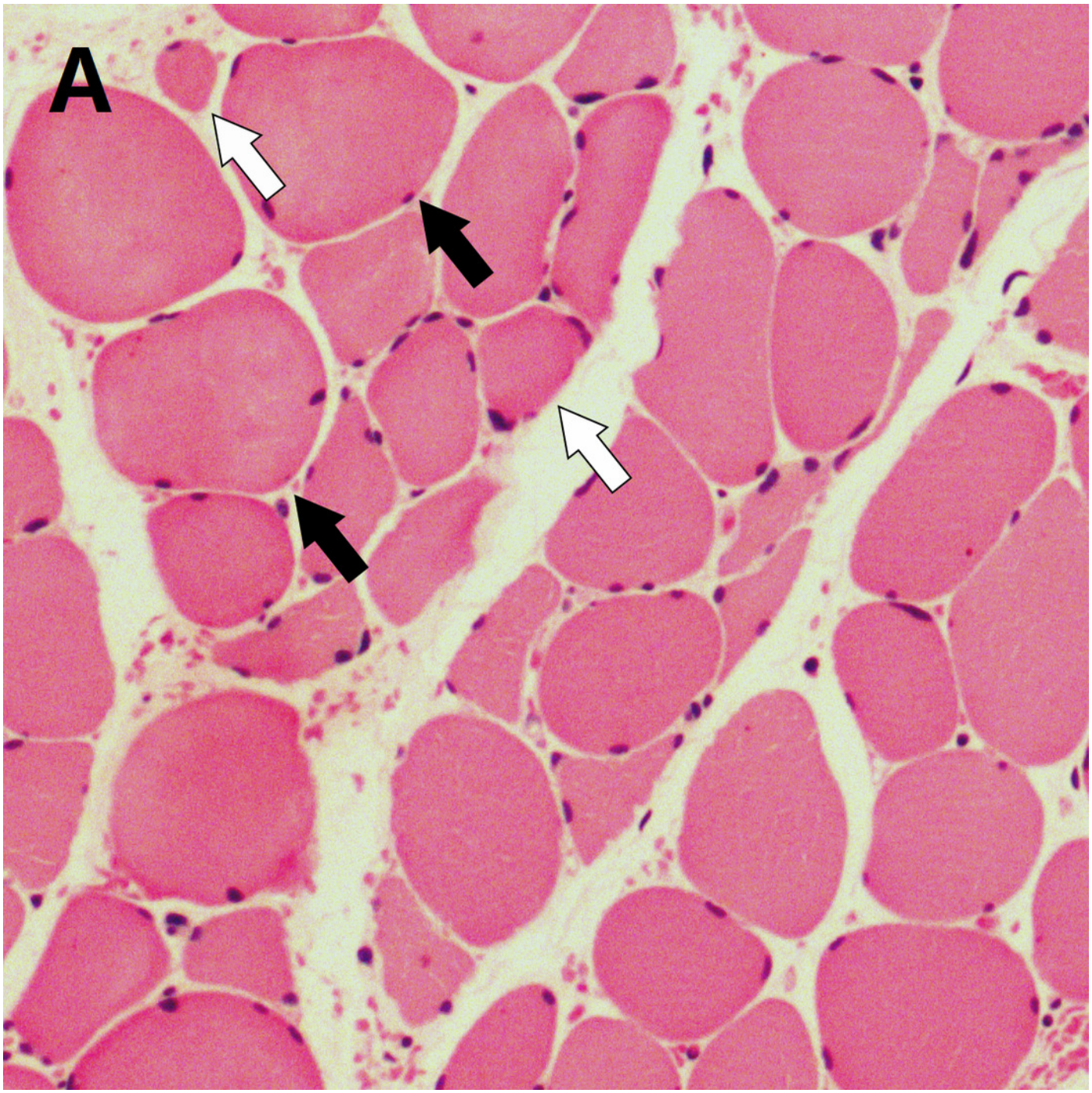
A

Figure 10

Microscopic views of muscle fibers from two groups of rats with HE staining (400×)

The histological changes of MTrPs are depicted in (A) (cross-section) and (B) (longitudinal section), which show that muscle fibers became thinner at both ends and swelled in the middle to show the contraction nodules in longitudinal section along with local muscle fiber gap widening. The histologically normal muscle fibers are similarly shown in (C) and (D), which reveal that the size and shape of muscle fibers are uniform.

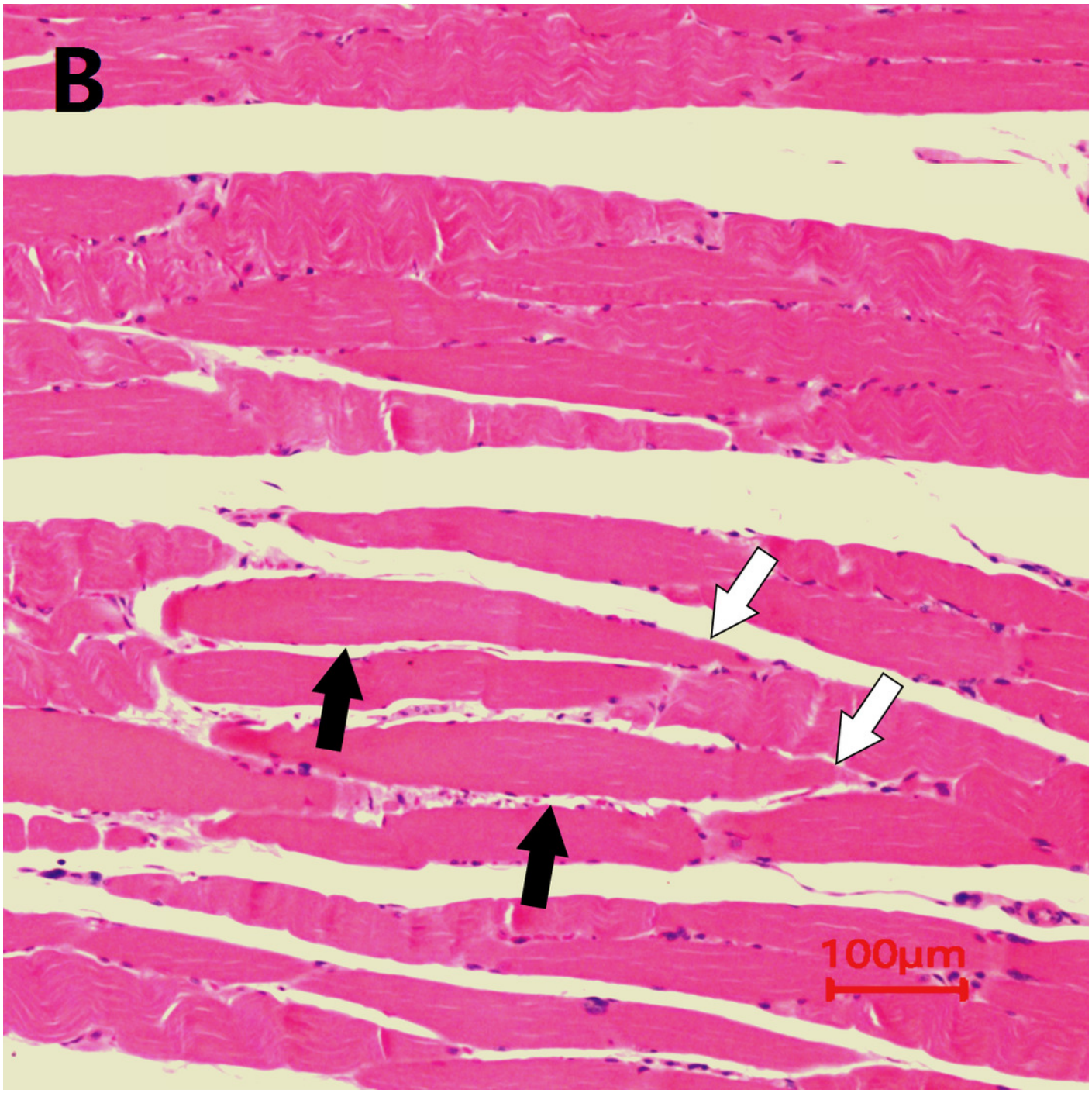
B
100µm

Figure 11

Microscopic views of muscle fibers from two groups of rats with HE staining (400×)

The histological changes of MTrPs are depicted in (A) (cross-section) and (B) (longitudinal section), which show that muscle fibers became thinner at both ends and swelled in the middle to show the contraction nodules in longitudinal section along with local muscle fiber gap widening. The histologically normal muscle fibers are similarly shown in (C) and (D), which reveal that the size and shape of muscle fibers are uniform.

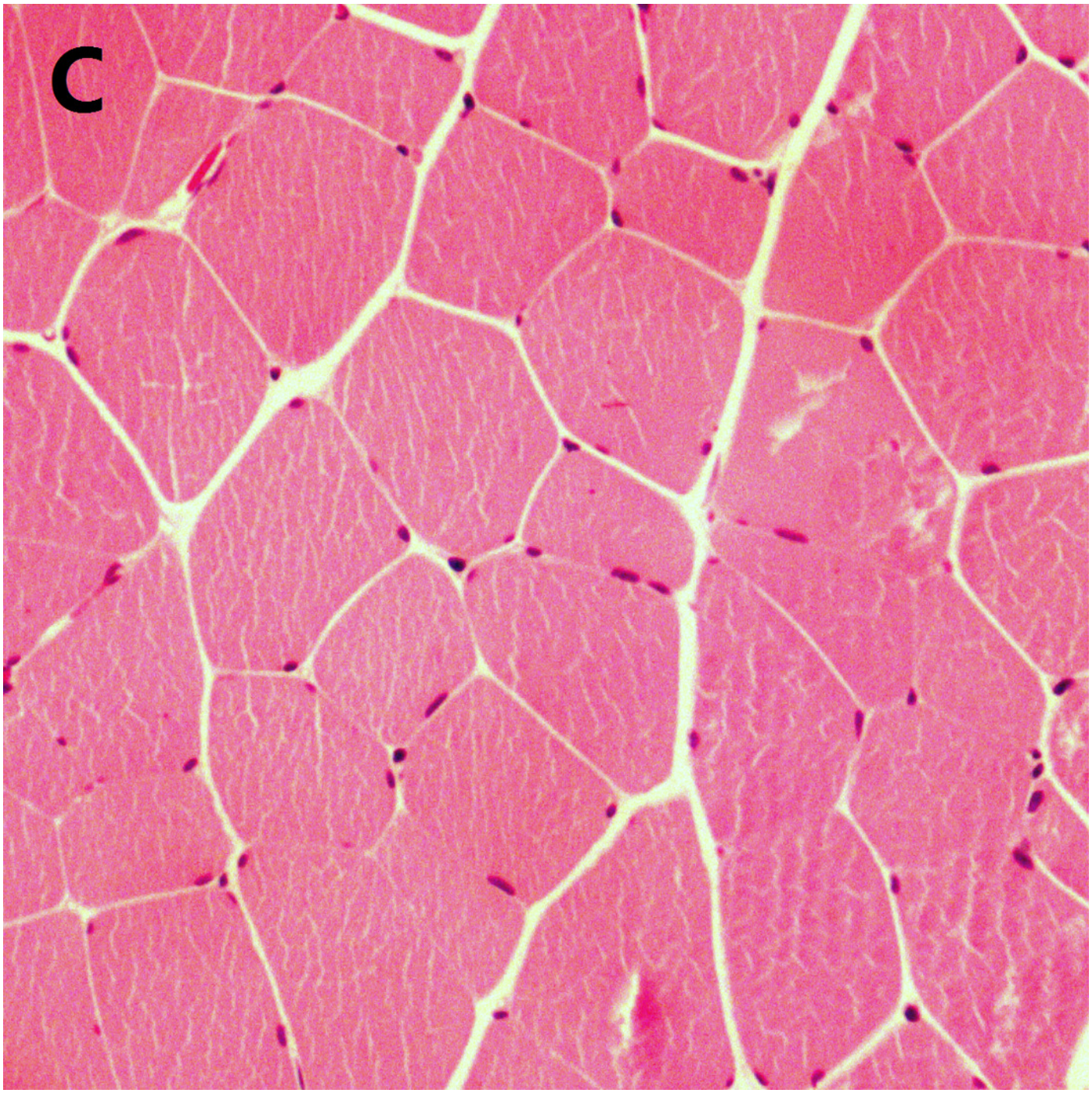
C

Figure 12

Microscopic views of muscle fibers from two groups of rats with HE staining (400×)

The histological changes of MTrPs are depicted in (A) (cross-section) and (B) (longitudinal section), which show that muscle fibers became thinner at both ends and swelled in the middle to show the contraction nodules in longitudinal section along with local muscle fiber gap widening. The histologically normal muscle fibers are similarly shown in (C) and (D), which reveal that the size and shape of muscle fibers are uniform.

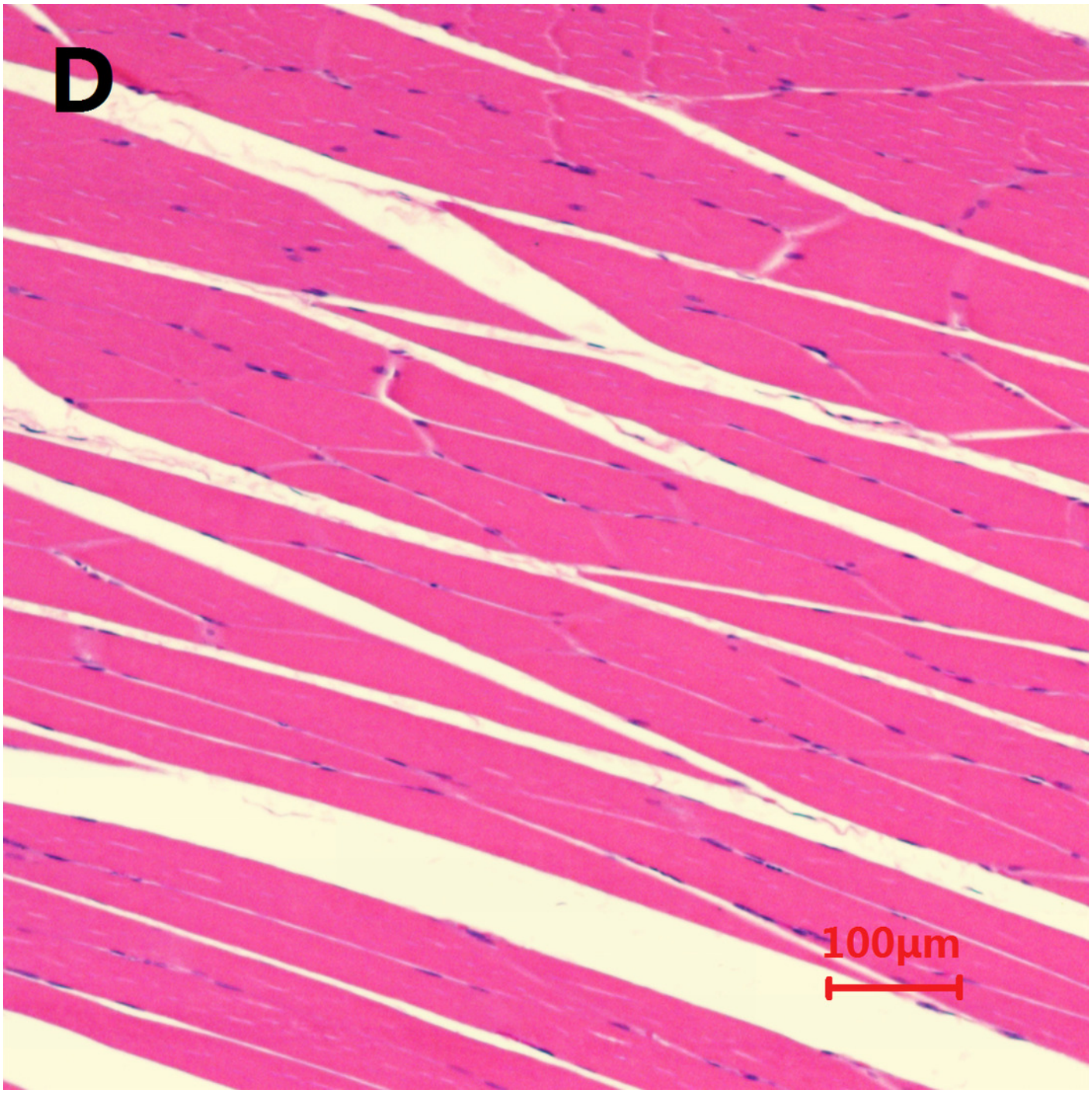
D
100μm

Figure 13

Comparison of the MVD in rat muscle fibers between the MTrP rats and normal controls

(A) and (B), Expression of CD31 detected by IHC in rats from the control group and the MTrP group, respectively. (C)Comparison of the MVD in rat muscle fibers from the two groups; *, $P < 0.001$.

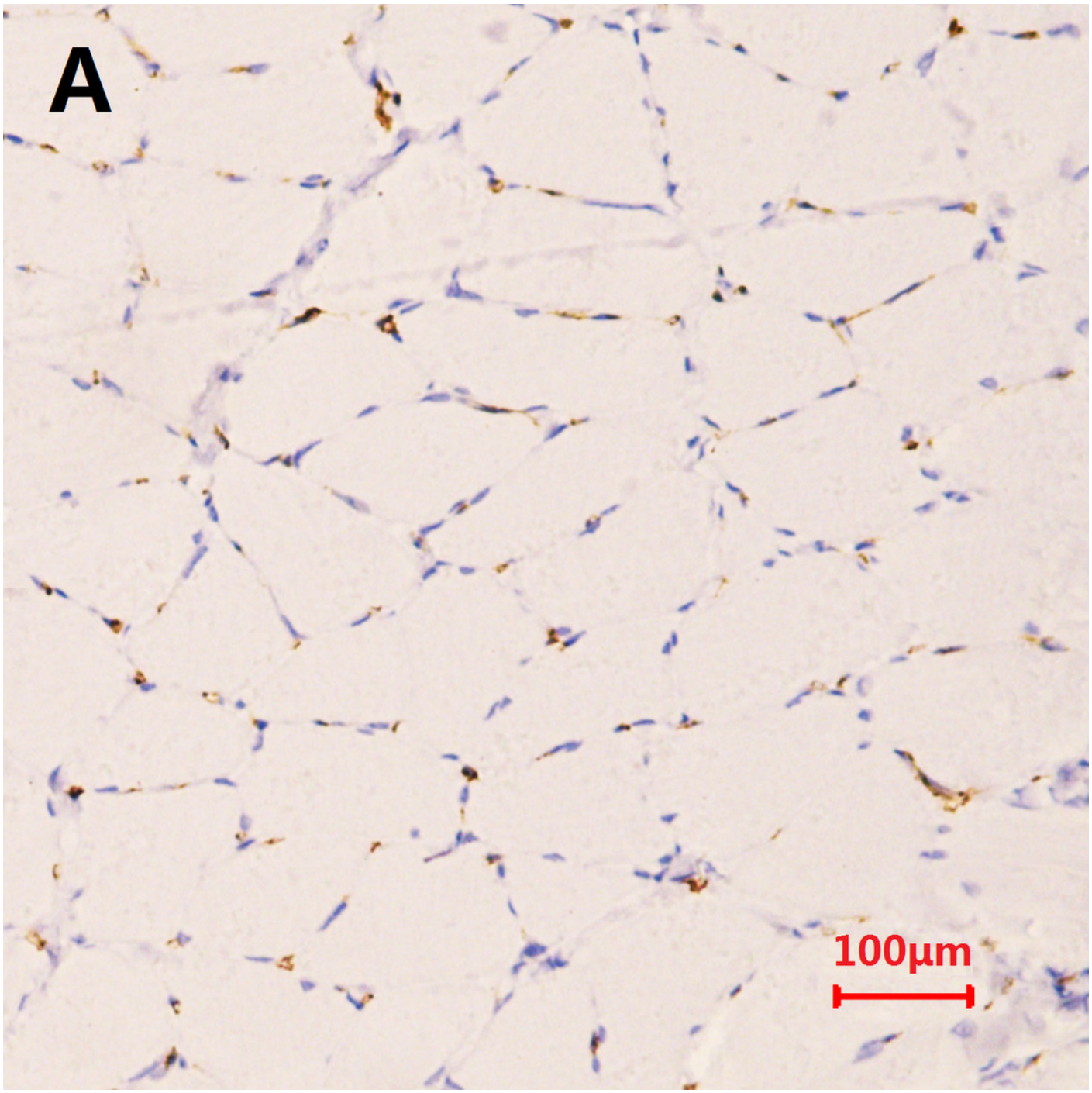
A
100μm

Figure 14

Comparison of the MVD in rat muscle fibers between the MTrP rats and normal controls

(A) and (B), Expression of CD31 detected by IHC in rats from the control group and the MTrP group, respectively. (C)Comparison of the MVD in rat muscle fibers from the two groups; *, $P < 0.001$.

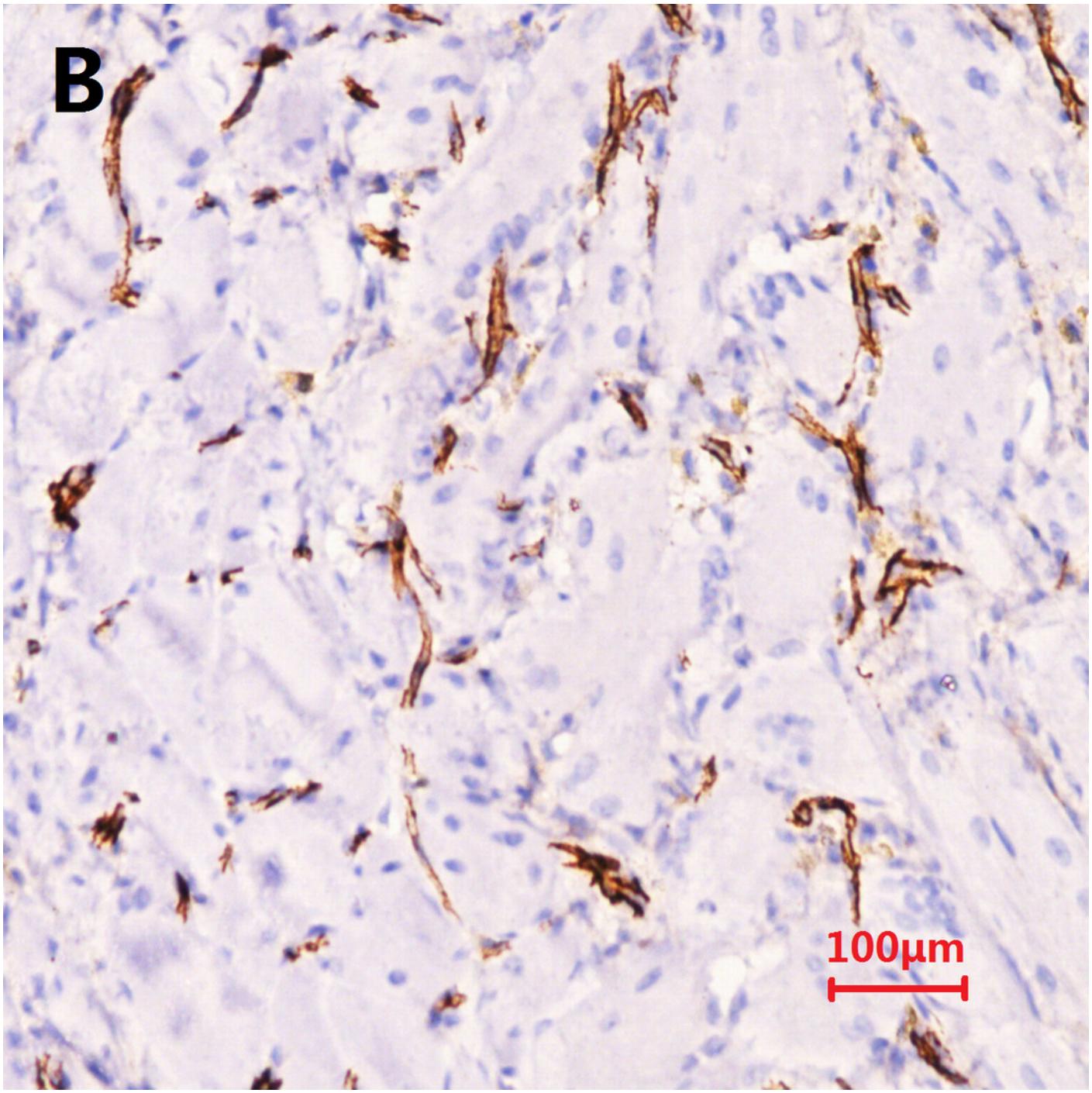
B
100µm

Figure 15

Comparison of the MVD in rat muscle fibers between the MTrP rats and normal controls

(A) and (B), Expression of CD31 detected by IHC in rats from the control group and the MTrP group, respectively. (C)Comparison of the MVD in rat muscle fibers from the two groups; *, $P < 0.001$.

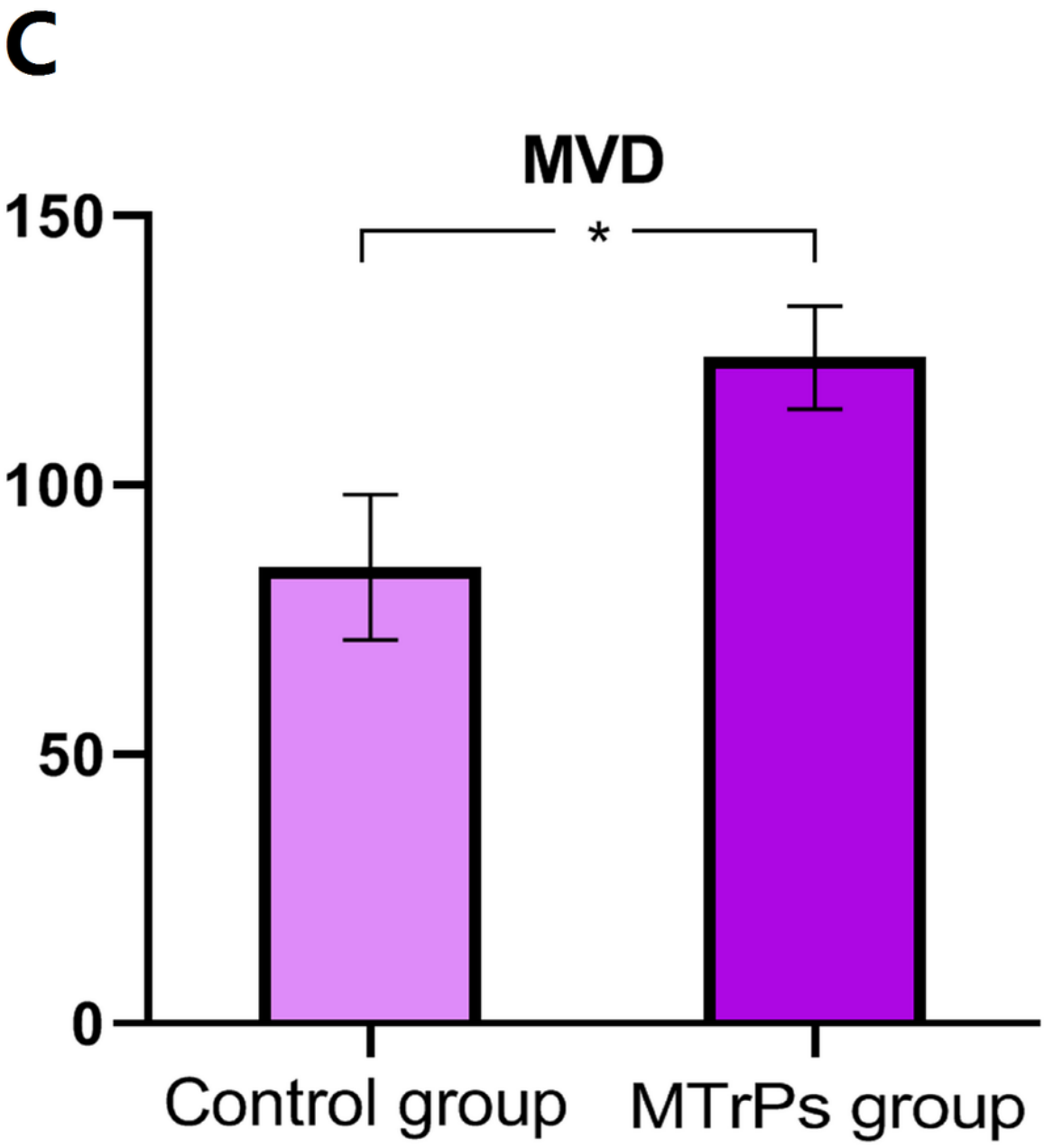
C
MVD
*
150
100
50
0
Control group
MTrPs group

Figure 16

Expression of HIF-1α and VEGF in two groups of rats.

* indicates a significant difference between the MTrPs group and normal control group *(P* < .001).

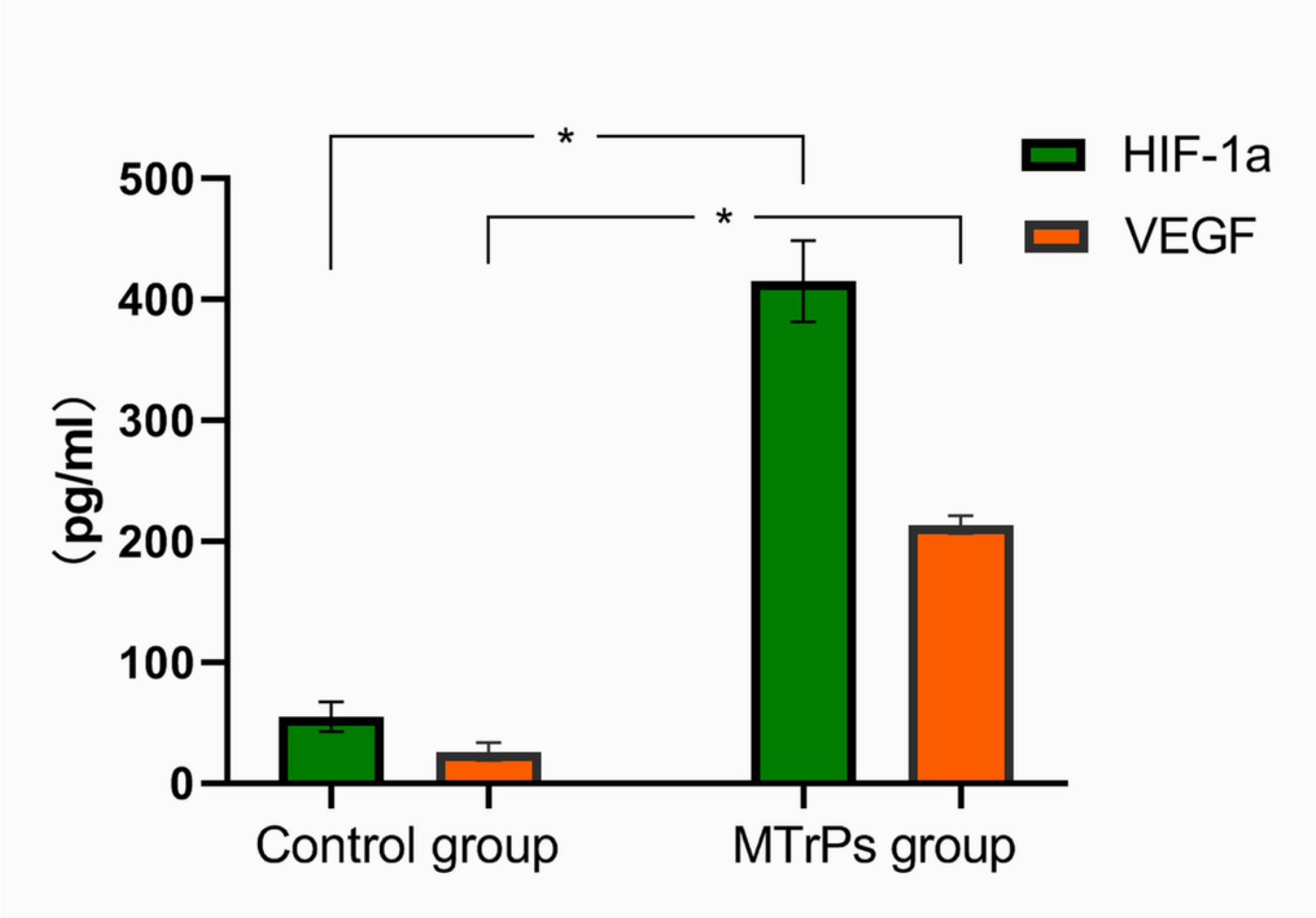

Table 1(on next page)

Results of blood flow signal grading

1 Table 1. Results of blood flow signal grading.

Grade	Criterion	No.(n=14)
0	No blood flow signals	2
I	One or two dot-like blood flow signals	5
II	Three dot-lik or a thin- and short-like blood flow signals	4
III	One or more large and longer blood flow signals	3

2

Table 2(on next page)

Correlation analysis of the parameters in the MTrP group

1 Table 2. Correlation analysis of the parameters in the MTrP group

Parameters	Grade of the blood flow signal Correlation coefficient	*P*
HIF-1a	0.403	0.154
VEGF	0.595	0.025
MVD	0.707	0.005

2